5G Communication with a Heterogeneous, Agile Mobile network in the Pyeongchang Winter Olympic CompetitioN

Grant agreement n. 723247

Deliverable D6.1
Access and backhaul: Integration and system testing

Date of Delivery:	30 Oct 2017
Editor:	Marko Leinonen
Associate Editors:	
Authors:	Tommi Kallio (Nokia), Jaakko Leinonen(Nokia) Aki Korvala (Nokia) Marko Leinonen (UOULU) Giuseppe Destino (UOULU), Olli Kursu (UOULU), Ilgyu Kim (ETRI), Junhyeong Kim (ETRI), Heesang Chung (ETRI), Gosan Noh (ETRI), Bing Hui (ETRI), Young-Min Choi (CL), Yongsoo Na (HFR), Sungmin Cho (SKT), Dongha Kim (SMRT)
Dissemination Level:	PU
Security:	Public
Status:	Draft
Version:	V0.2
File Name:	5GCHAMPION_D6.1_Final.pdf
Work Package:	WP6

	Title:	Deliverable D6.1Access and backhaul: Integration and system testing.	
	Date: 20-10-2017		Status: working document
	Security: Public		Version: V2.0

Abstract
This deliverable provides integrated and functionally tested wireless backhaul HW. HW that will be used in 2018 Olympics to demonstrate 5G capabilities.

Index terms
5G, mmWave, algorithm, beamforming.   **<u>Inputs:3.5 document, WP2.1 and WP2.2 documents</u>**

Contents

List of Acronyms

3GPP	3rd Generation Partnership Project
5G	5th Generation
5GTN	5G Test network
AGC	automatic gain control
BB	Baseband
BRU	Backhaul Radio Unit
CA	Carrier aggregation
dBi	decibel isotropic
EIRP	Effective isotropic radiated power
EU	European union
GaN	Gallium nitridi
HW	hardware
IF	intermediate frequency
KPI	Key performance indicator
KR	Korea
LNA	low noise amplifier
LO	local oscillator
LoS	line-of-sight
MIMO	Multiple-input-multiple-output
MME	Mobility Management Entity
MMIC	monolithic microwave integrated circuit
mmW	millimetre wave
MUX	Multiplexer
OIP	output intercept point
PA	Power amplifier
PCB	Printed circuit board
PoC	Proof of Concept
QAM	Quadrature amplitude modulation
QPSK	Quadrature Phase Shift Keying
RF-DFE	Radio Frequency Digital Frontend
RSSI	Received signal strength indicator
SDN	Software defined networking
SNR	Signal-to-Noise Ratio
TDD	Time Division Duplex
WP	Work package

Table of Figures and Tables

1 Introduction

This is a document that describes the integration and system testing results of KR side wireless backhaul proof of concept(POC) and EU mmw POC intergation.

Document is divided so that first version, 1.0., will cover only integration results of POC. This is due the delays in antenna board manufacturing which then prevents the overall system testing to be performed. Then version 2.0.0 will cover the whole system testing results for POC system that will be demonstrated in Olympics 2018. So telling the maturity of system and KPI´s.

First version is done by end of june 2017(M13) to cover integration aspects and by November 2017 M18 system testing results will be added. Before M18 this document is stored to 5GChampion internal database.

2 Key components of the EU mmWave transceiver platform

Following picture describes the building blocks of EU 5G RF building blocks. More information from D3.5 document.

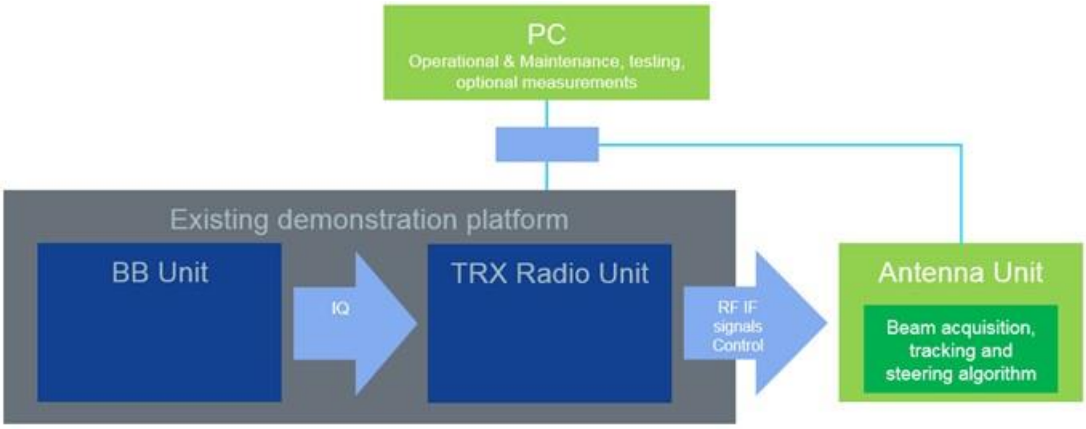

Figure 1: EU POC key components

2.1 Overview of architecture of transceiver platform

EU mmW transceiver consist of L2 CPU and 10Gbps switch, baseband, digital front end, RF and antenna parts.

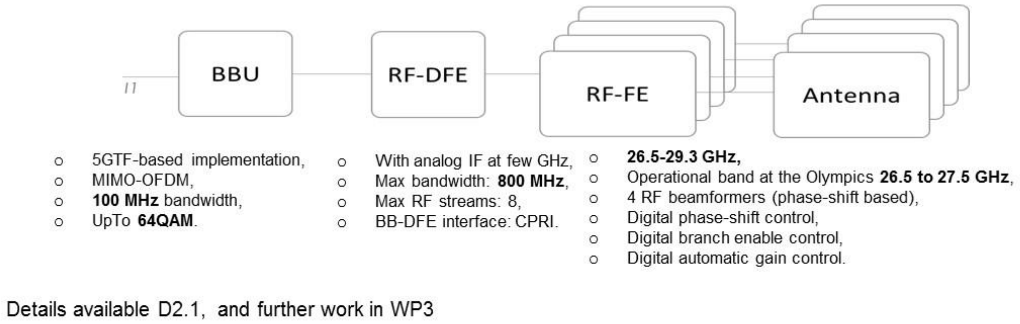

Figure 2 : EU POC architecture

More information from D3.5 document.

2.2 Overview of antenna unit

Following chapters 2.2.1 and 2.2.2 are adopted from document [2].

2.2.1 RF architecture and block diagram

The RF architecture and implementation is targeted for a mobile backhaul working in the frequency band of 26.65-29.12 GHz (frequency range used in Korea in the planned location for the P-o-C demonstrations). The mobility brings more requirements with respect to conventional backhaul including beam steering and the requirement to manage farfield/nearfield problem with varying signal levels at receiver. To get the range the maximising the output power at transmitter is important.

The selected RF beamforming architecture is based on phase-shifters and linear antenna array providing 2D beamforming. The size of the array and corresponding array gain is the trade-off between the available power from the PA, physical dimensions coming from the number of PAs and array physical size and effective isotropic radiated power (EIRP).

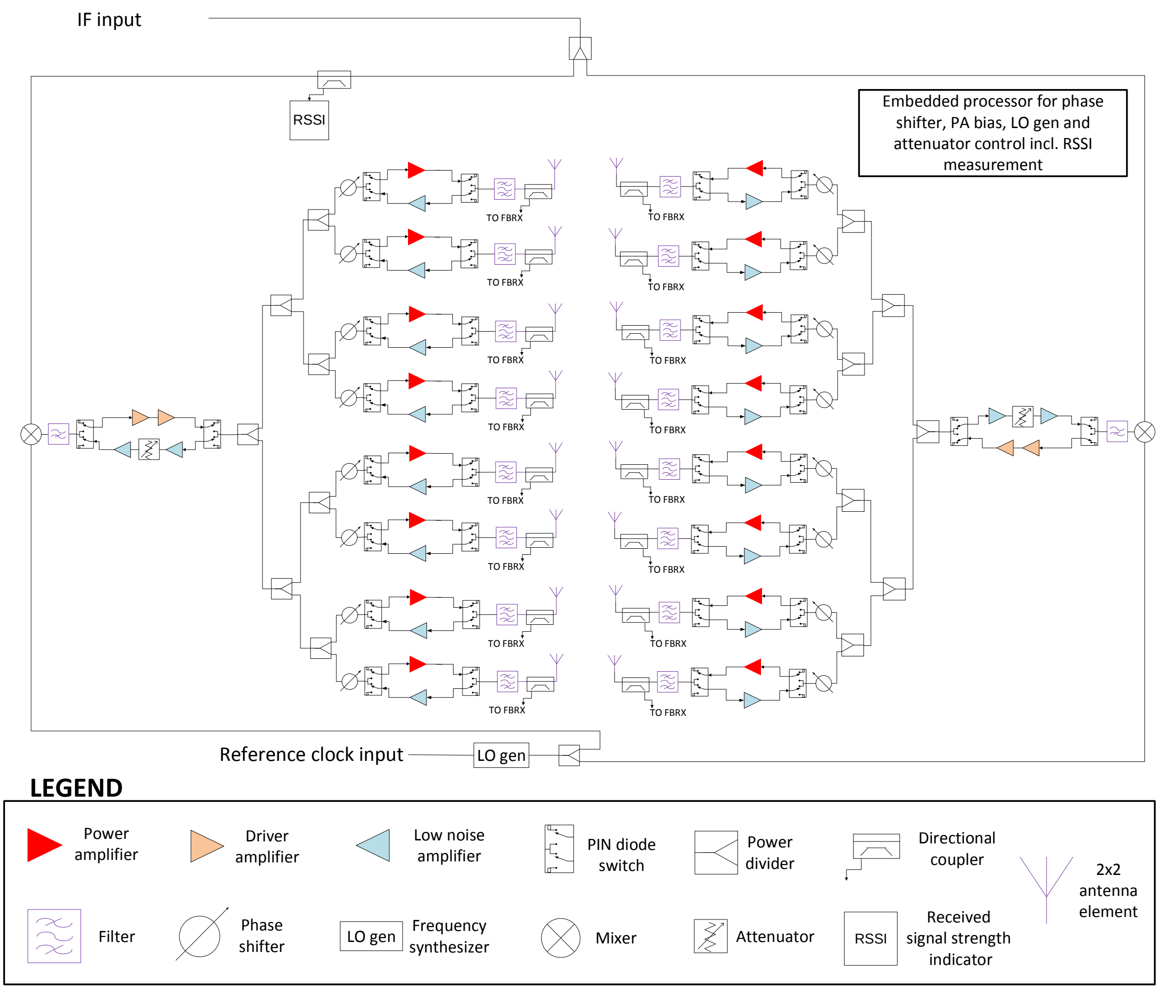

Figure 3: Block diagram of one transceiver channel.

The front-end electronics hardware shown in Figure 3 implements the RF signal paths from the intermediate frequency (IF) to final transmitter frequency fed into inputs of antennas. Since we have TDD system where the transmitter and the receiver are not operating at the same time, we have implemented a partially shared signal path and shared antennas for the transmitter and the receiver. The transmit (TX) and receive (RX) modes are separated by using p-i-n diode switches.

On the transmit path the following functionality is implemented:

- Power division of IF signal to two separate paths,
- Frequency transition to final RF frequency using mixer for which LO-signal is fed from frequency synthesizer (LO-gen),

- Signal amplifying before feeding to distribution network implemented by power dividers,
- Signal phase shifting independently in each RF branch,
- Signal amplification by power amplifier (PA) before,
- Signal filtering before feeding to antenna element.

On receiver path the following functionality is implemented:

- Signal filtering after antenna,
- Signal amplification using low noise amplifier (LNA),
- Signal phase shifting using phase shifter,
- Signal combination from different antenna branches using power combiners,
- Signal amplification and gain control,
- Frequency transition to intermediate frequency IF.

Signal distribution to the phased array antenna is implemented in two parts due to practical printed circuit board implementation which targets to locate each driving PA as close to antenna subgroup as possible. Two parts share the same LO but have own mixer and amplifier paths.

The radio implementation is done in two phases where the first phase named v1 is a radio board with eight transmission and reception paths which are shown in the Figure 3. The second phase radio board named v2 includes all shown radio circuitries of the block diagram shown in Figure 3.

2.2.2 Antennas

The linear phased array of 16 2x2 sub-elements was selected to fulfil the requirements used in link budget calculations presented in report IR2.1 [1].The early simulations shown in Figure 4 indicate that it is possible to achieve antenna gains around 22dBi as used in link budget calculations. This is preliminary performance used in system calculations.

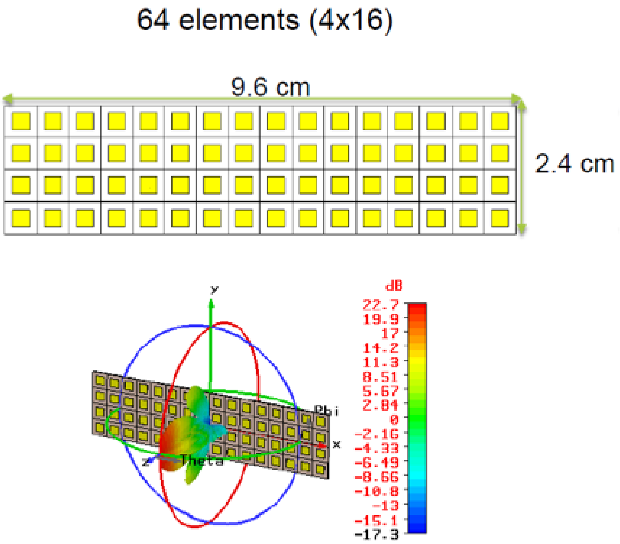

Figure 4: Linear phased array and radiation pattern at 26.5GHz frequency

An antenna array is developed and manufactured based on simulations and a picture of the full 16 port antenna array is shown in Figure 5.

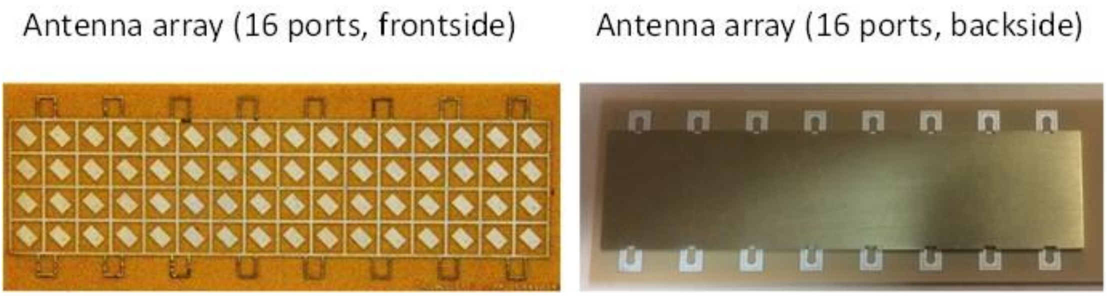

Figure 5: Manufactured antenna array with 16 RF ports

3 Access and backhaul: Integration and system testing results

3.1 L2 integration to EPC

Used PoC system uses IP-tunneling between applications and L2 protocol in BTS and UE. No real EPC is used but EU PoC can use whatever IP source including EPC as a source. Note that no control nor user plane of 4G/5G is not used.

3.2 BB and TRX integration

Baseband HW is implemented in FPGA based architecture. TRX HW is also implemented based on FPGAs. FPGA based solutions enables SW based PoC style approach. This enables modularity to the system and helps the future implementation of SoC based solutions.

Connection between BB and TRX is implemented with CPRI cables. Synch and data between BB and TRX is communicated with CPRI protocol.

TRX board handles DFE and RF implementation, including AD/DA conversions. From TRX signal is send with RF cables towards the antenna elements.

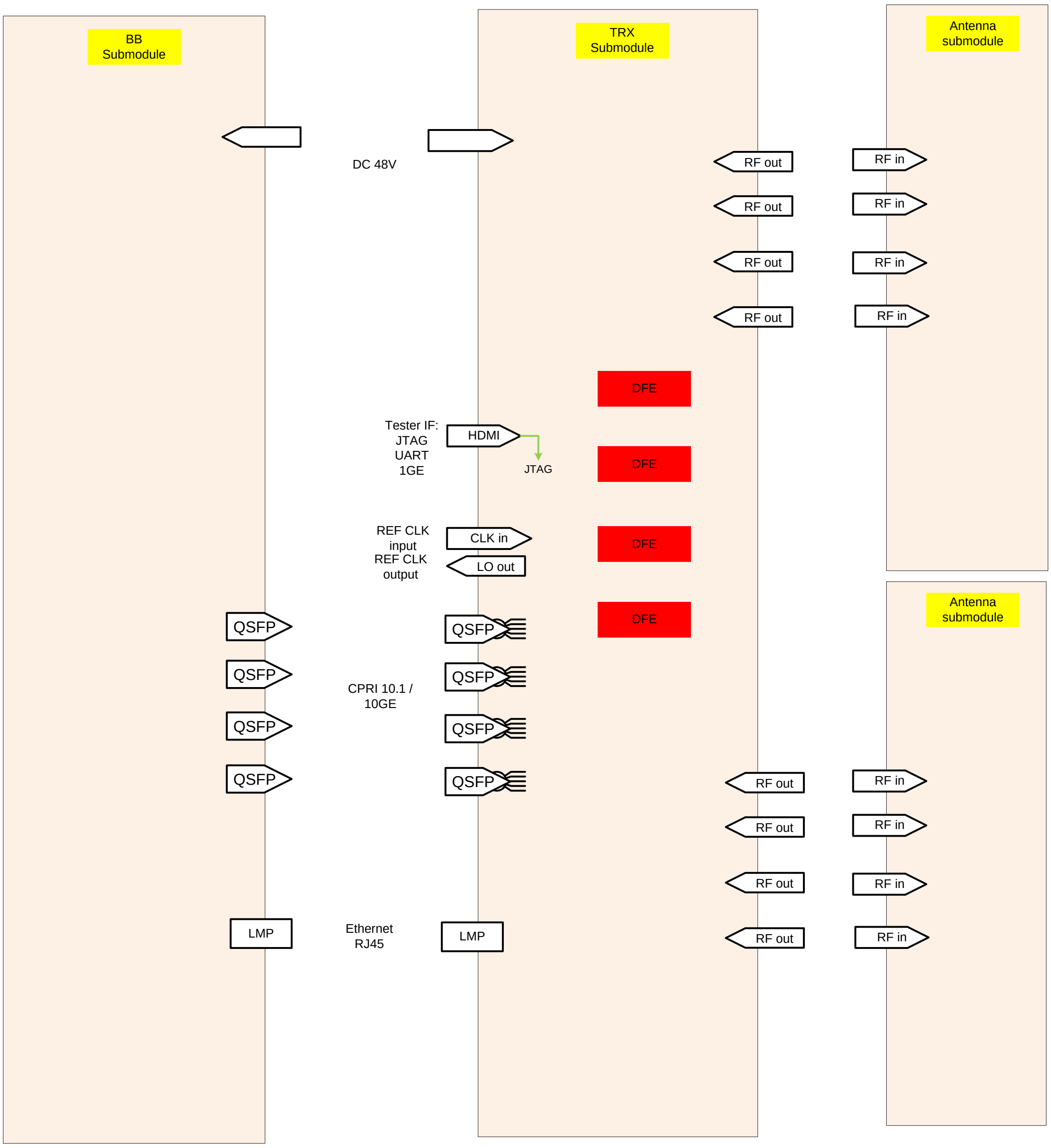

Figure 6: BB, TRX and antenna

Integration of the BB and TRX boards is executed with help of internal test vector generating in BB module. FPGA releases on BB and TRX boards are tested by generating test signal in BB and observing the sent signal from TRX modules RF outputs with signal analyser.

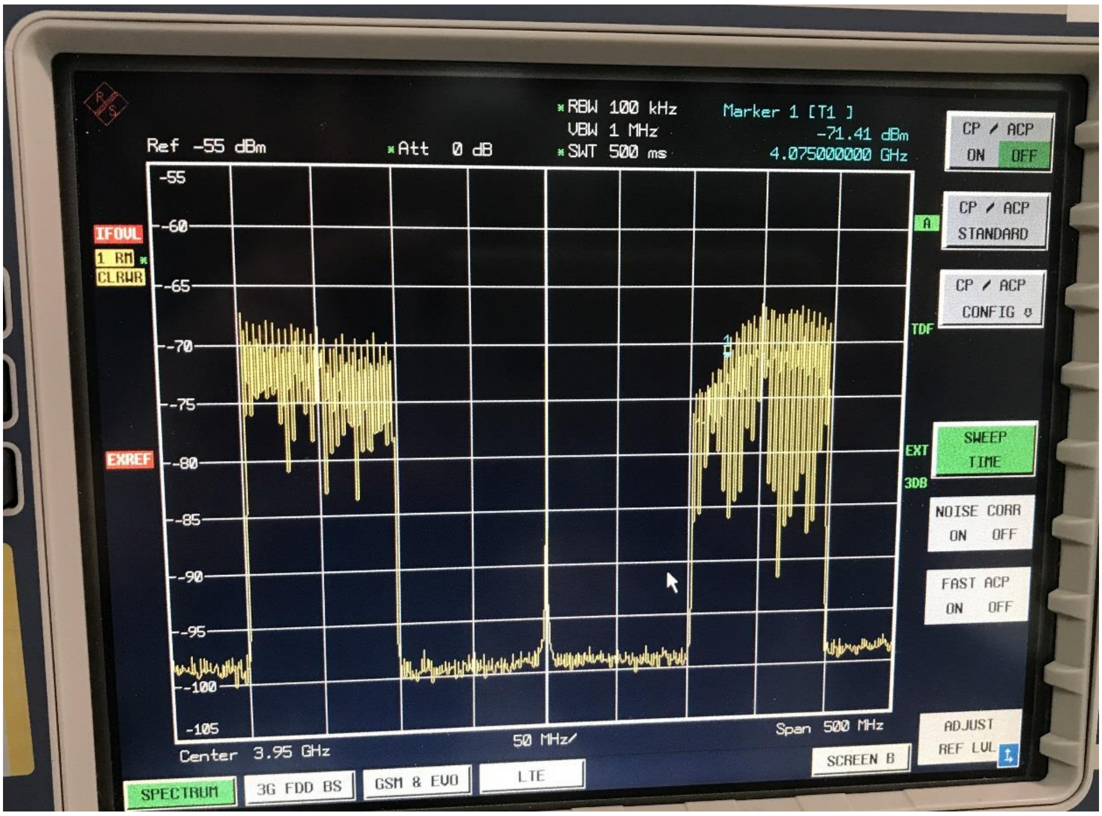

Figure 7: TRX IF output signal

3.3 TRX and Antenna unit integration V1 board

Unit integration testing has been performed for the radio board V1 without BB functionality, thus integration has been focused to the radio functionality and radio performance. Real radio performance can be evaluated and tested with true BB signal and absence of real signal test signal has been used in radio testing.

A 100MHz wide OFDM signal was not available from the available laboratory test system equipment and thus a single carrier test signal has been used. Radio testing has been carried out with a 100MHz wide single carrier modulated (16QAM and 64QAM) test signals. This signal is not exactly similar as 100MHz wide OFDM signal, but this signal gives a good view the performance of the radio solution. A spectrum figure of the test signal is shown Figure 8.

Figure 8: Example of test signal: 100MHz single channel 16QAM modulated signal

An overview picture of the test system is shown Figure 9 which includes main measurement equipment which are used in radio integration. This same measurement equipment setup may be used for receiver and transmitter testing with different configuration.

The overview picture includes at least following measurement equipment which are used for radio integration:

- A computer to run a signal generation software (SW)
- Arbitrary waveform generator for generate baseband test signal
- RF signal generator with IQ-input from arbitrary waveform generator
- RF signal generator to generate reference signal for Device Under Test (DUT) and rest of the test system
- Vector Signal Analyzer (VSA) to demodulate the test signal
- DC power supplies for operational voltages

Vector signal analyzer has been used to analyze a quality of the received signal for the first radio board, since real base band was not available for tests. The received signal quality is measured with Error Vector Magnitude (EVM) which includes amplitude and phase behavior of the receiver of the DUT.

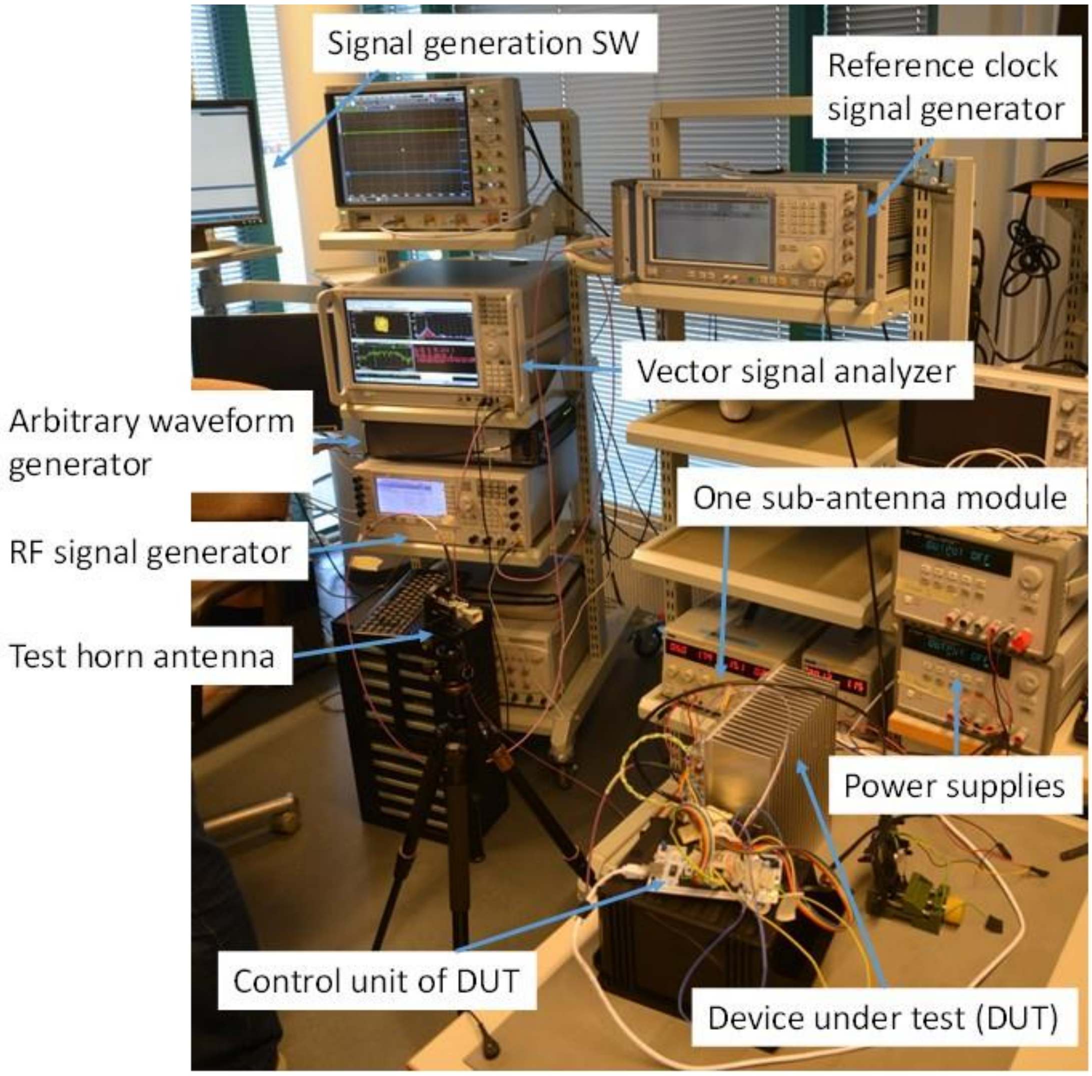

Figure 9: Overview picture of the integration test system for first radio board

Test configurations for receiver testing are shown Figure 10. Test signal generation for the receiver testing is done with following method. The test system includes a signal generation software which generates test signal for an arbitrary waveform generator. The arbitrary waveform generator generates for example a 100MHz wide 16QAM modulated baseband signal which is routed to a RF signal generator. The RF signal generator coverts the baseband signal to a RF frequency for example 26.5GHz.

A test signal is fed to the DUT with a coaxial cable for conductive tests or with a reference test antenna for radiated tests. The radio board receives RF signal and amplify and converts it to an Intermediate Frequency (IF) which is selectable with software which operates DUT. As an example 4GHz IF is shown in the Figure 10.

There are two different kind of radiated tests which may be performed with a radio card. The first is to connect one sub-array for one RF receiver path and the second is to connect a full antenna module to all reception paths.

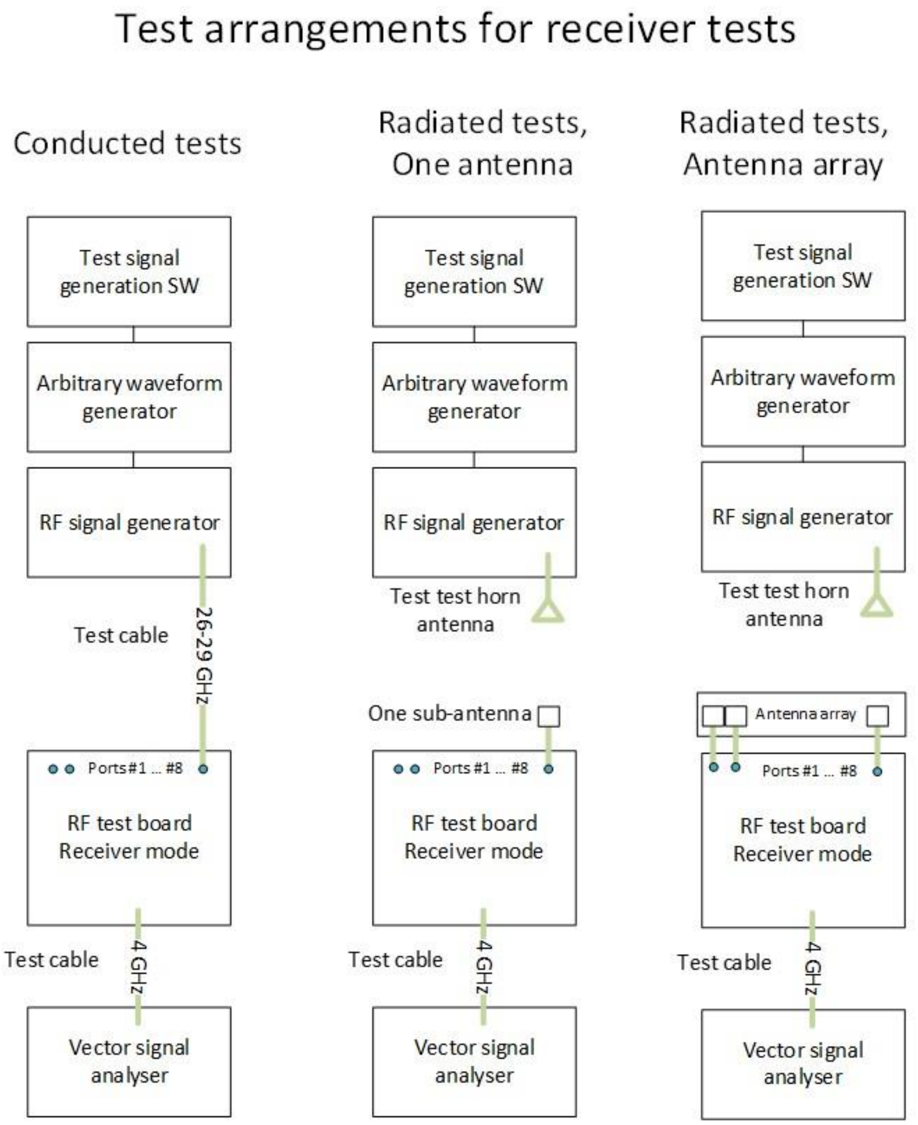

Figure 10: Test system configurations for receiver testing

Conducted and radiated tests with one sub-antenna have been conducted with first radio board. Conducted receiver EVM tests for each receiver paths have been done and measurements have been done with VSA. Example of EVM measurement results is shown in Figure 11EVM measurement result curves at 26.5GHz from some receiver paths are shown Figure 12. These EVM figures are measured with constant amplitude and phase settings. EVM curve raises with high power levels due to non-linearity of the receiver. EVM performance with low signal levels is limited due the noise level of the receiver. There are deviations between receiver signal paths due to component variations.

Figure 11: EVM measurement results at vector signal analyzer display

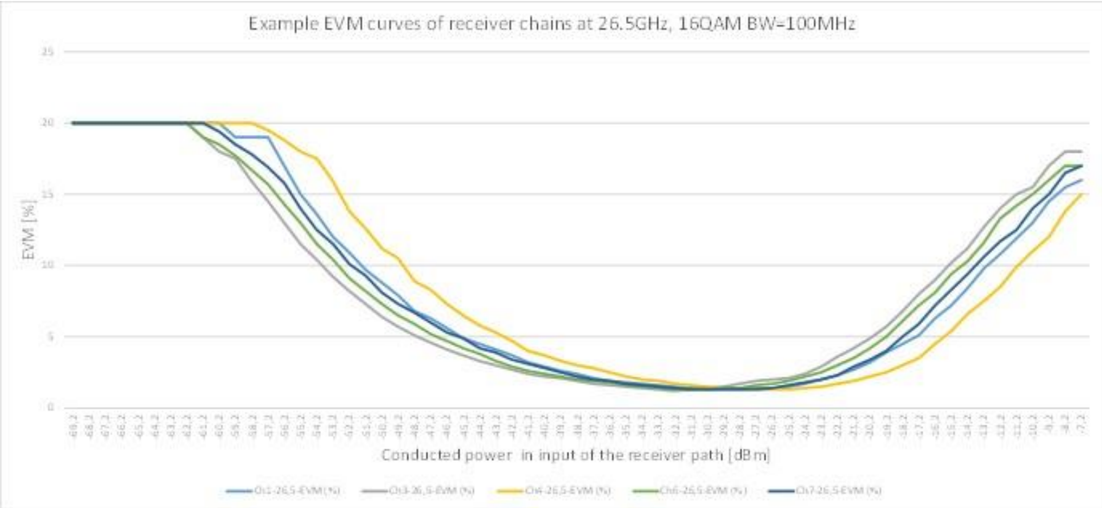

Figure 12: Example receiver EVM curves of receiver paths measured at same frequency

Transmitter testing can be done with the same measurement equipment than receiver testing and an overview of transmitter testing is shown in Figure 13. Transmitter testing system is similar to receiver test system up to RF signal generator. IF signal is fed to the IF input of the radio transmitter which is converted to RF frequency with DUT. The transmission signal is amplified with the transmitter and it is fed to antenna connector. The antenna connector may be connected with coaxial cable to spectrum analyzer or vector signal analyzer for conductive testing or alternatively to the antenna for radiated testing.

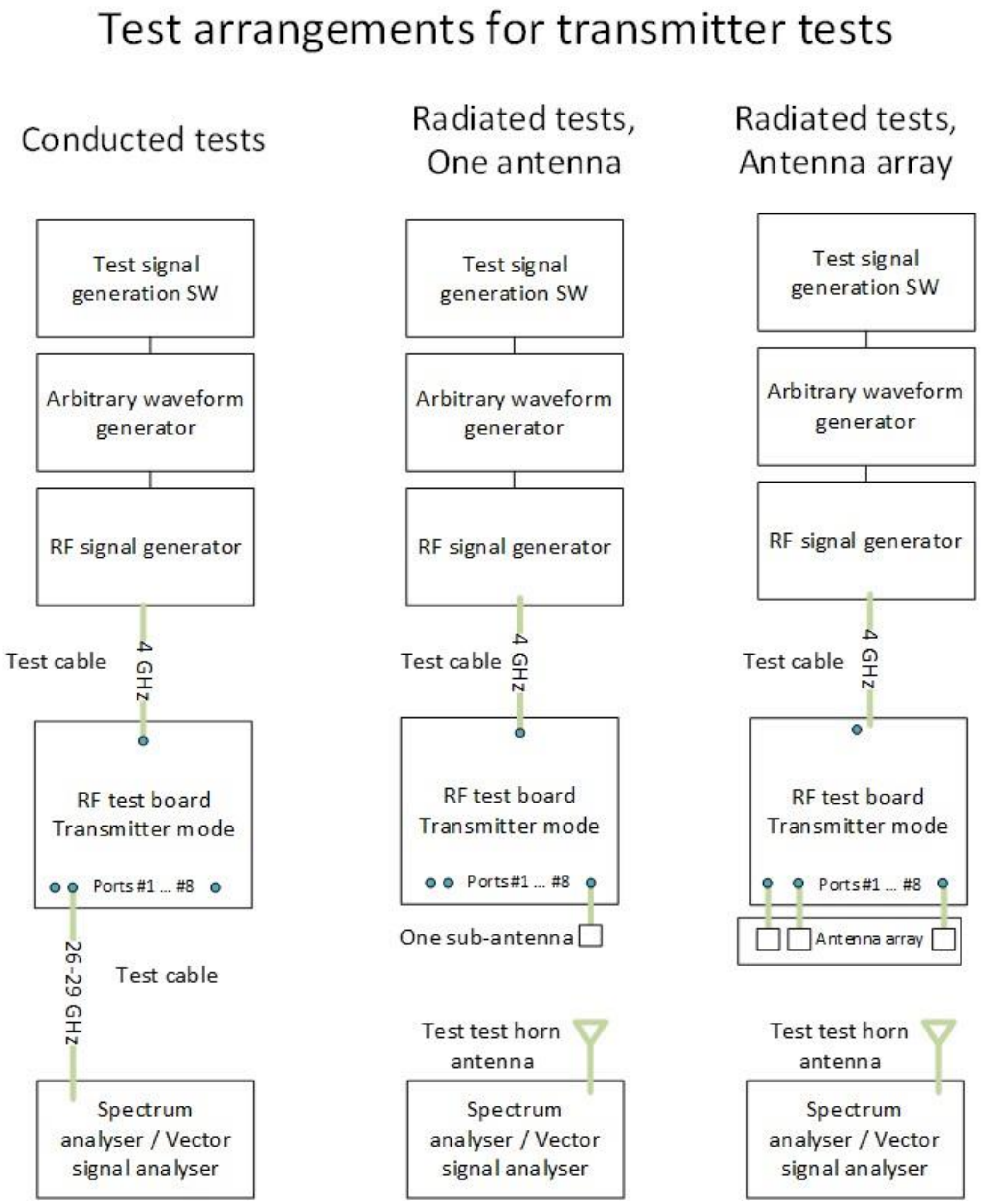

Figure 13: Test system configurations for transmitter testing

Conductive testing has been done for first radio board and example test results is shown in Figure 14. The transmission power from the transmitter of the first radio board is lower than expected due unwanted oscillation of the power amplifier. The result shows that at least +17dBm linear transmission power can be delivered to the antenna connector.

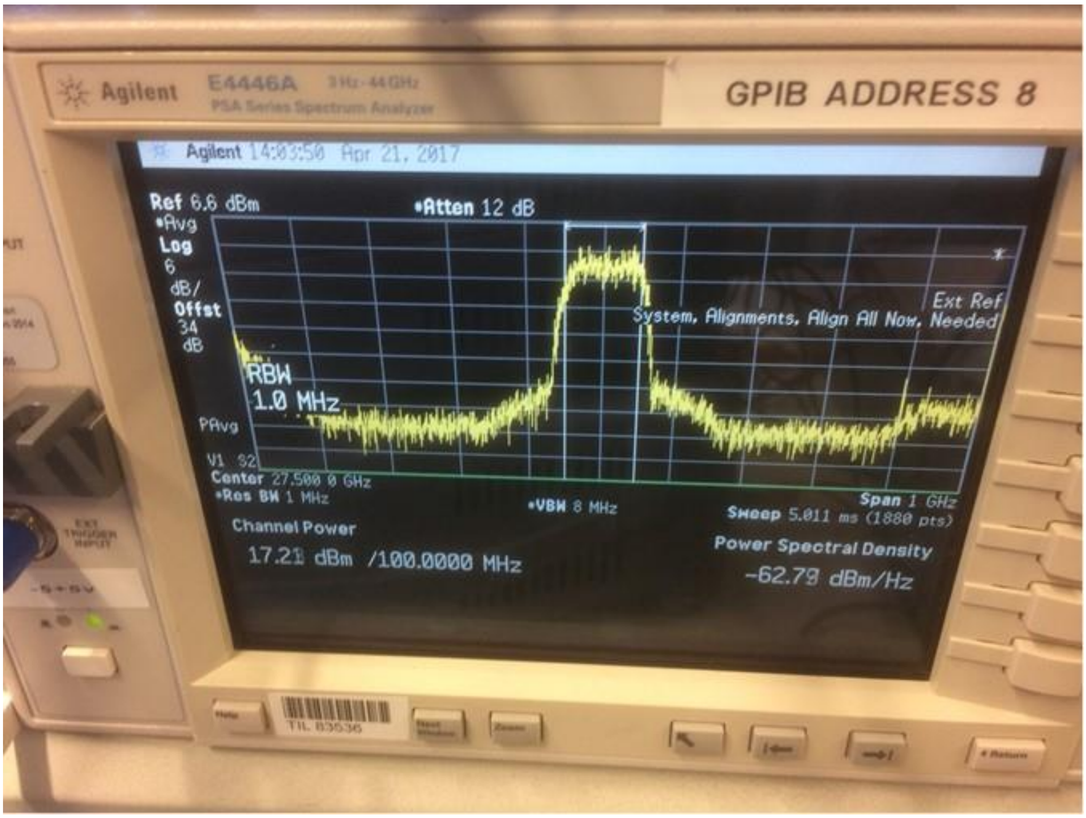

Figure 14: Spectrum of the transmission of first radio board with 16QAM 100MHz wide test signal

3.4 TRX and Antenna unit integration and system testing

3.4.1 System testing with v1 radio board of antenna unit

System level testing have been done based on the system configuration presented in Figure 6. Receiver functionality of the whole radio system has been tested and a photograph of the used configuration is shown inFigure 15.

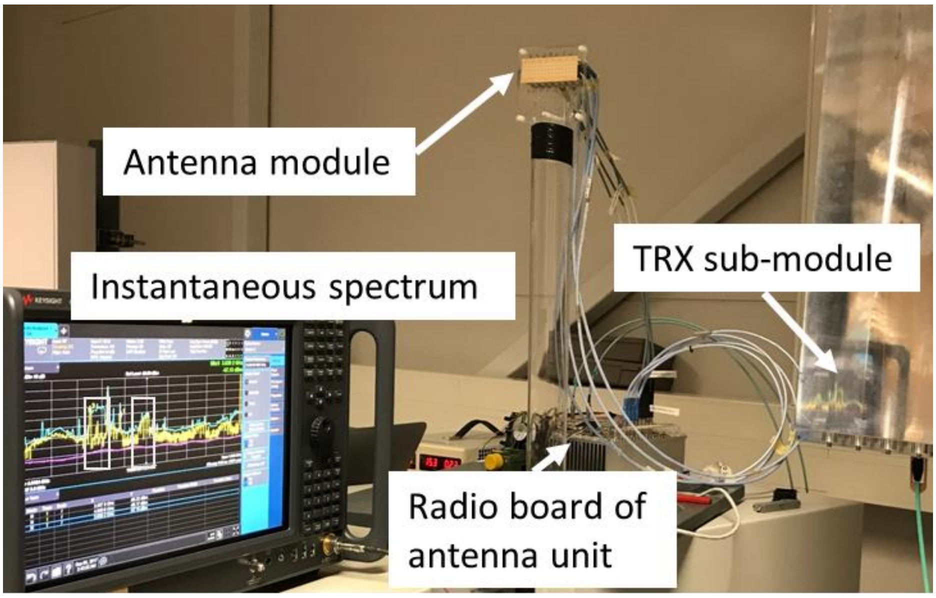

Figure 15: Photograph of the whole radio system testing

Measurements of the whole radio system were carried out as an over-the-air measurement as shown in Figure 10. The transmission of the signal was taken from other antenna unit operating at 26.7GHz and two transmitted signal was received with the v1 radio board. The antenna which is connected to the v1 radio board is the same as shown in Figure 5. Cables between the antenna module and the radio board have been used to have flexible installation during the tests.

Instantaneous spectrum during the measurement is shown in the figure 15 in the spectrum analyzer. Light grey boxes at the spectrum are highlighting the communication signals.

Some spurious signals below the communication signals were caused by the non-linearity of the receiver and those were improved by changing settings of the transmitter unit.

Signal levels of the reception were measured and those matched to the expected signal levels based on the transmission power of the transmission unit and distance between units.

Effect of the polarization was measured and 16dB polarization effect was detected to the level of the received signal.

Transmitter of the v1 radio board was not tested in a full radio system testing due to radio component failure of the board.

3.4.2 System testing with v2 radio board of antenna unit

Manufacturing of the v2 board have been postponed from original time schedule and thus integration results v2 are not available at time of writing.

Results of v2 board system integration will be in IR6.1 document [3].

4 KR mmWave backhaul: Integration and system testing results

The Korean wwWave backhaul system is designed to support Gbps wireless data backhauling between NodeB (mNB) and terminal equipment (mTE) installed on a vehicle. The NB consists of multiple digital units (mDUs) and its corresponding radio units (mRUs). The TE also consists of a baseband (BB) unit and its corresponding RF and antenna module. The mmWave backhaul system is connected to the public internet via GW (EPC). Figure 16 shows KR mmWave wireless backhaul system.

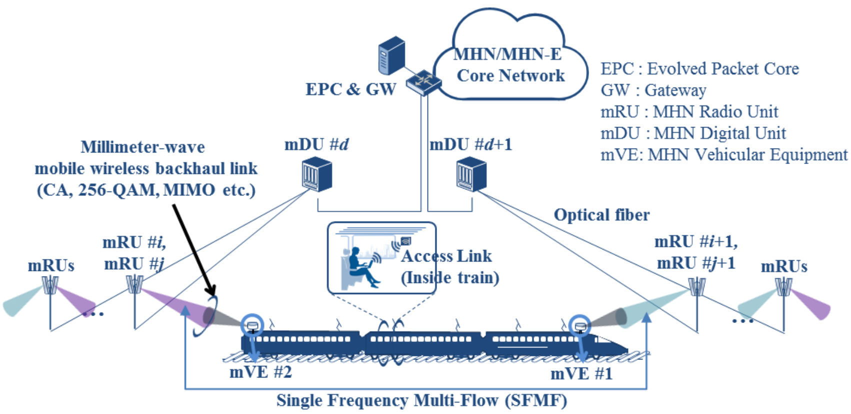

Figure 16: KR mmWave wireless backhaul system

4.1 GW (EPC) of KR mmWave wireless backhaul system

Figure 17 shows the core part architecture of KR mmWave wireless backhaul system. This system support S1AP Interface, S1 handover, packet routing and forwarding, DPDK for high rate and massive contents packet processing, GTPv2 Encapsulation/De-capsulation.

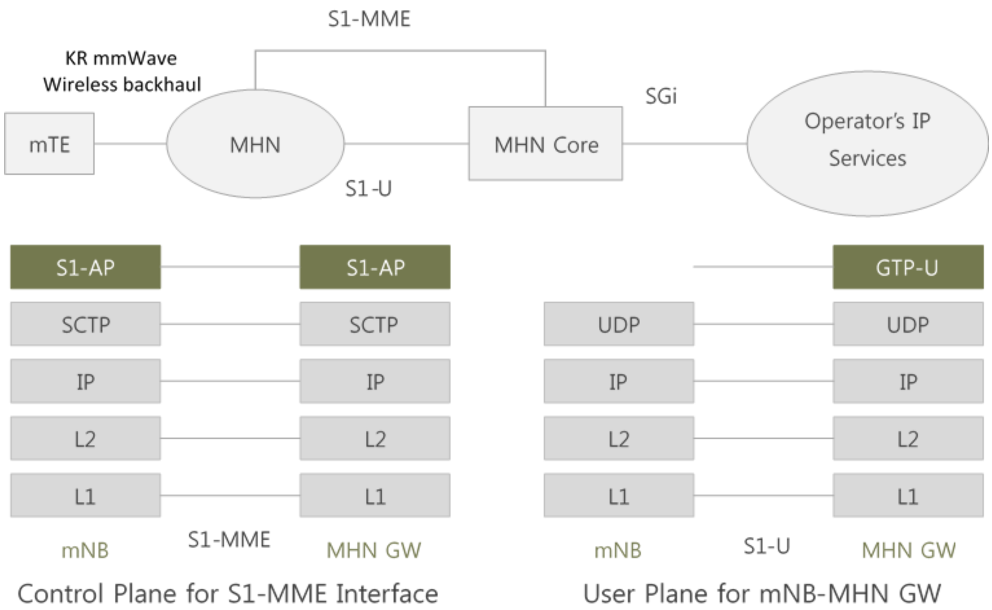

Figure 17: Core part achitecture of KR wireless backhaul system

The mobile wireless backhaul core is divided into control unit and data unit by function. All signal processing functions are integrated into the control unit and traffic processing functions are integrated into the data unit. The GW is implemented to provide high-speed / high-capacity packet processing using Intel's NIC and DPDK solution. Control unit and data unit, divided by function, are developed based on a flexible structure, which is easy for capacity expansion and performance expansion according to increase of traffic capacity. Figure 18shows high rate and massive contents packet processing concept based on DPDK. The basic properties are

- Handle traffic separated from the Kernel of the OS using Intel's NIC and DPDK Solution
- Intel's high-performance CPU dedicated to traffic processing
- Support up to 5 Gbps of traffic per mTE session
- Expansion memory and CPU is easier than network process card, where CPU and memory are fixed
- Distributed processing structure of work core for efficient traffic processing

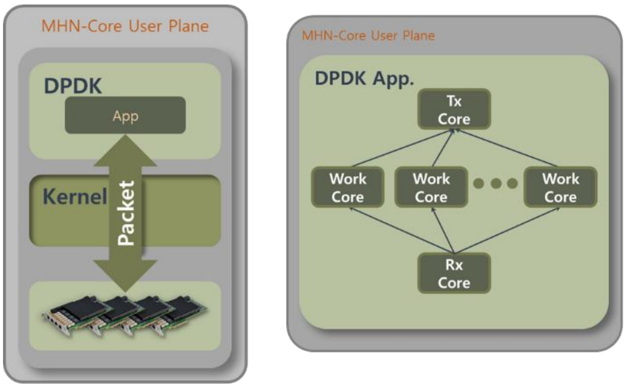

Figure 18: DPDK for high rate and massive contents packet processing

4.2 Modem and BB platform of KR mmWave Wireless backhaul

Figure 19 and Figure 20 show the architecture of mDU and mTE MODEMs. The mDU MODEM consists of several sub-modules including TrCH encoder, TrCH decoder, downlink modulator, and uplink demodulator. Similarly, the mTE MODEM consists of several sub-modules including TrCH encoder, TrCH decoder, uplink modulator, and downlink demodulator. Additionally, the mTE MODEM includes the front-end controller and cell searcher. For both mDU and mTE MODEMs, interfaces to the corresponding L1 controller are configured. Additionally, the mTE MODEM also provides control signaling for the antenna module. Figure 21 shows the BB platforms for the mDU and mTE. The BB platforms include the FPGAs which contain modem RTL logic. Both platforms also include AD/DA and DIF module. There are also CPU (MPC T2081) for L1 control SW. Figure 22 shows the high layer platform based on Intel Xeon. The interface between Xeon platform and BB platform is PCIe and the interface between Xeon platform and GW is 10G Ethernet.

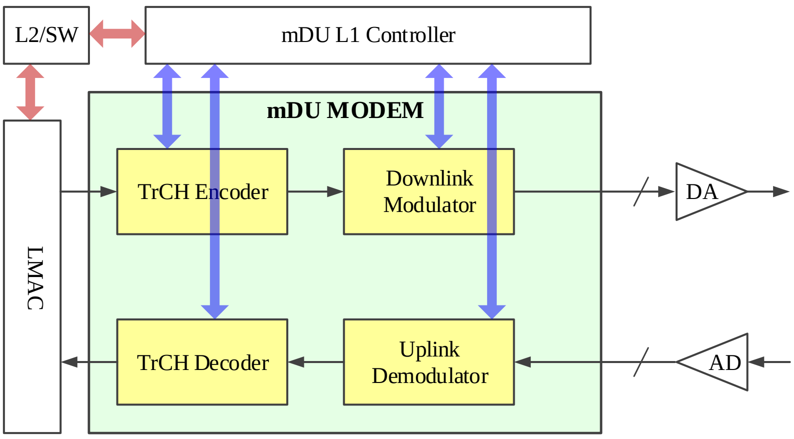

Figure 19: mNB/mDU MODEM architecture and interface to higher layer

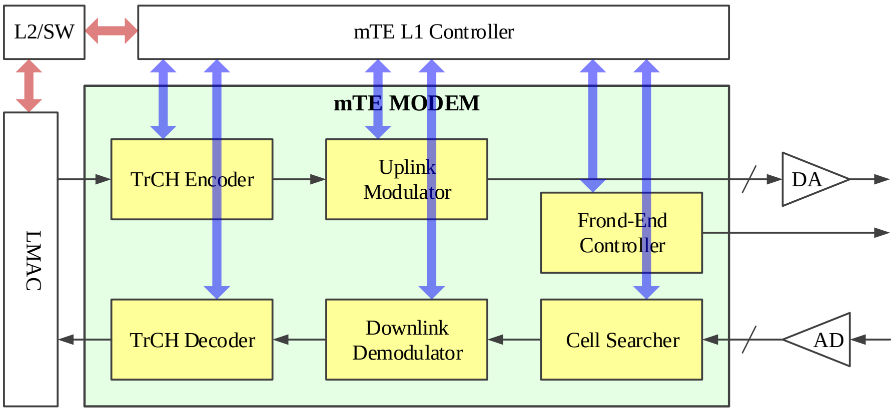

Figure 20: mTE Modem architecture and interface to high layer

Figure 21 NodeB (DU) Baseband platform and TE Baseband platform

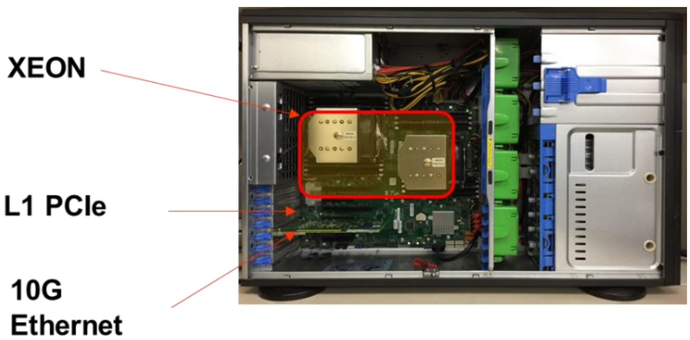

Figure 22: Platform for L2/L3 protocol stack

4.3 RF and antenna of KR mmWave Wireless backhaul

Figure 23 shows the layout of the MHN radio unit that includes two TRX modules and 2T2R antennas. A power supply module, local oscillator module and radio-over-fiber (RoF) interface module are included. The RoF interface is used to connect between the radio unit and corresponding baseband processing unit. The length of fiber between the two units is up to 5 km. The beamformers used in the radio units are all for fixed beam. Since the main applications of the MHN system are for high-speed or subway trains and their route are predetermined, the fixed beamformers can cover all the routes by appropriate cell configurations considering curved and straight paths. Figure 24 is the real HW of the TRX and antennas.

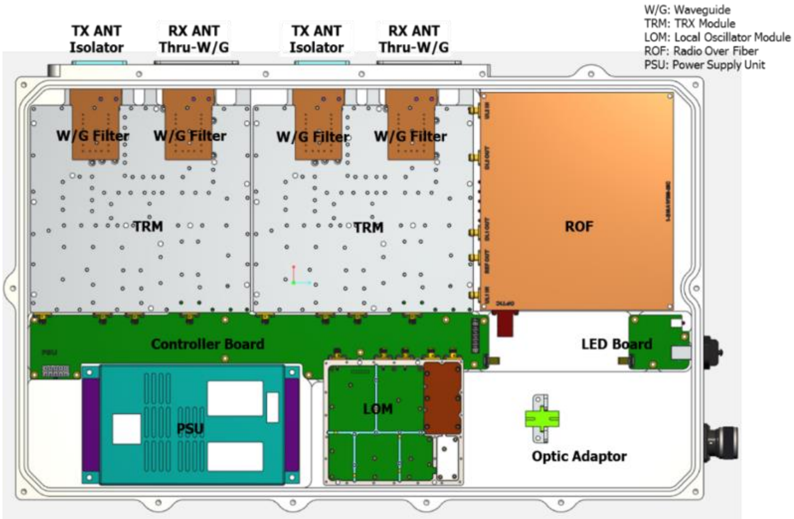

Figure 23: Layout of MHN radio unit

Figure 24: RF and Antenna Unit (RU)

4.4 Testing results

4.4.1 Indoor lab test

Functionalities of the MHN system are primarily tested under an indoor environment. A test setup is shown in Figure 25. An mNB consist of an mDU (Digital Unit) and an mRU (Radio Unit). An mTE includes a baseband part and radio part in a module. In the figure, higher layer protocol stacks such as MAC, RLC, PDCP, RRC and NAS are represented, but they are not mandatory in a physical layer link test. The setup is for maximum downlink capacity of 1.25 Gbps. For 2.5 Gbps of downlink capacity, we use two links as in Figure 26. The figure shows two sets of the test link depicted in Figure 26. One important point is that the two links are using the same carrier frequency. Though they have the same frequency, the interference to the neighbor link is not so big to deteriorate each link performance since they adopt directional beams with narrow beam widths. Figure 27 shows two displays representing diagnostic monitors for each link, respectively. Each peak data rate is larger than 1.25 Gbps so that the aggregated data rate is larger than 2.5 Gbps.

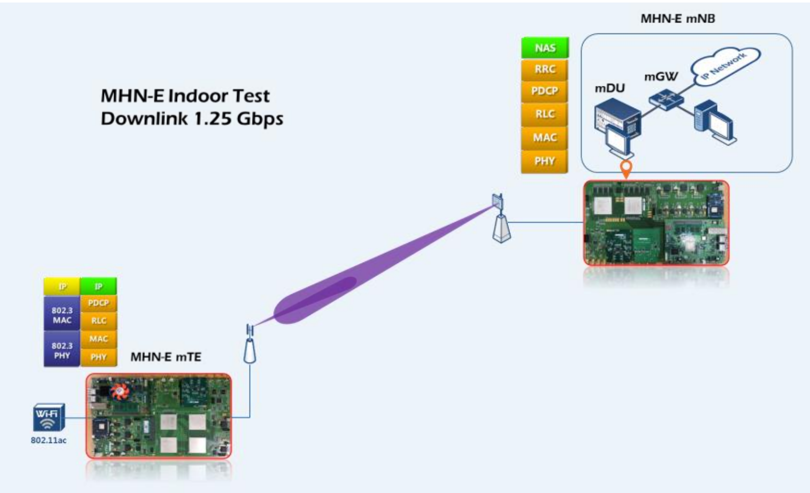

Figure 25: Concept of indoor link test setup

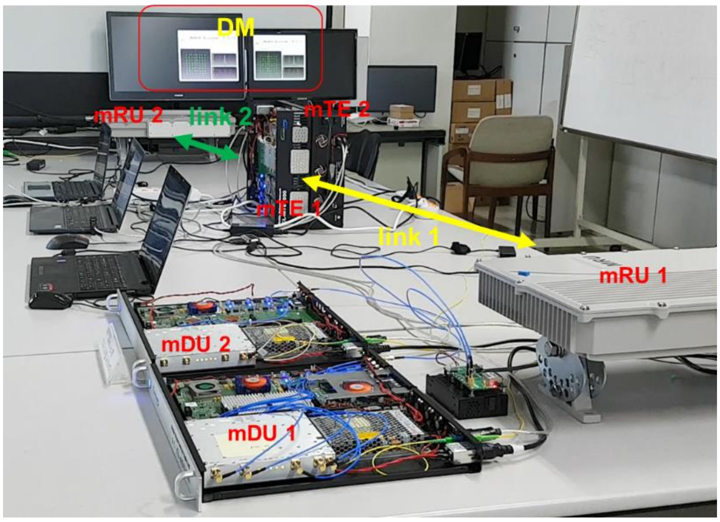

Figure 26: Picture of test setup for indoor link

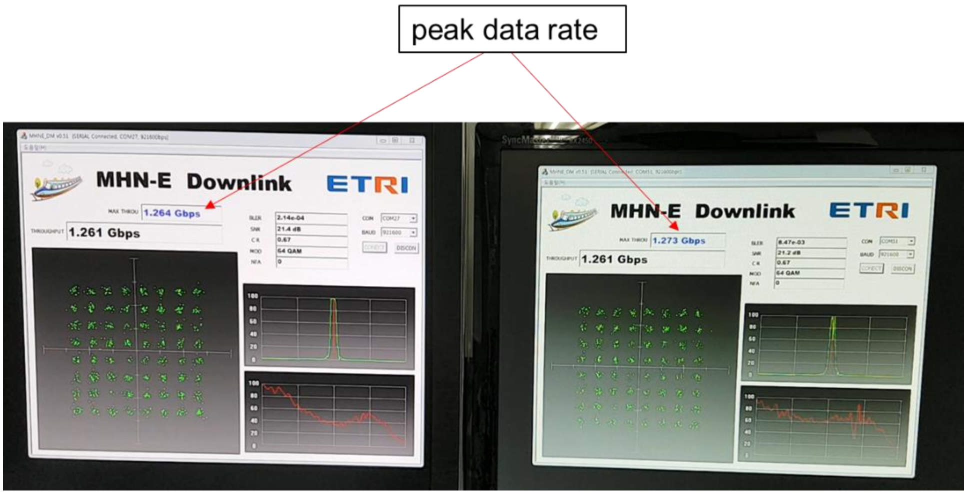

Figure 27: Peak data rates in diagnostic monitors

4.4.2 Subway field test

Real environments for the subway or high-speed trains are different from the indoor environment in many ways. First of all, the trains run under various channel environments such as the tunnels, rural, urban, viaduct, stations, mountains, etc. Therefore, it is meaningful to demonstrate the functionalities of the MHN system in the real world. The tunnel among many environments is very challenging since it represents strong and fast fading channel characteristics.

In this regard, the MHN system has been tested in the running subway trains of Seoul subway Line 8. Figure 28 shows a train path of Seoul subway Line 8 where the MHN systems was tested. There are three stations, Jamsil, Seokchon and Songpa from left to right in the figure. Four mRUs were installed between the Jamsil st. and Seokchon St. to cover the curved path. An mRU was installed near the Songpa St. for the straight path. The locations of the five radio units were determined by a wave propagation test using mmWave-based MHN prototypes before this field trial. The specification and characteristics of the used equipment are explained in the earlier subsections. Figure 29 illustrates a picture of an mRU installed on the wall of the tunnel along the train route.

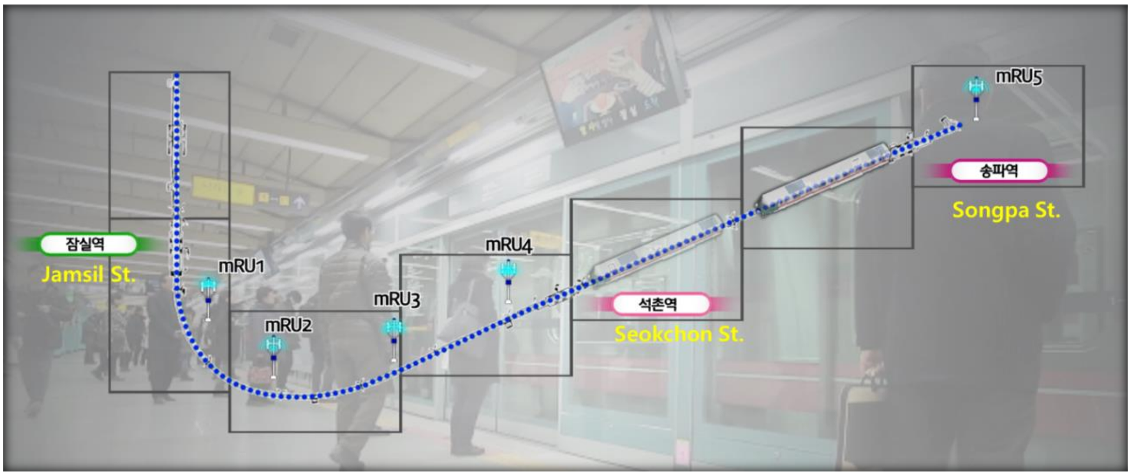

Figure 28: Seoul subway Line 8 path for a field trial

Figure 29: Picture of installed mRU

An mTE was installed in the engine room of the running train just behind the front window. If the mTE approaches the Jamsil St., it starts a random access to attach to the mNB. As the train runs through the route in the figure, the mTE receives and transmits signals from/to the mRUs on the nearest mRUs. When it passes the mRU, it carries out the handover procedure to connect to the next cell until it pass through the last mRU. Figure 30 illustrates a captured performance monitoring display that includes 64QAM constellation, frequency and time domain impulse responses and downlink and uplink data throughput. The green line (bottom) shows downlink data throughput. It keeps maintaining 1.25 Gbps of data rate most time. Four drop points indicate handover regions. In this field trial, the critical functionalities like handover and data throughput have been proven.

Figure 30: Measured performance of the MHN system in a field trial

4.4.3 Field test at Gangneung IoT Street

This subsection mainly describes a preliminary field test conducted along Yulgok Street, also known as IoT Street, in Gangneung city, Korea, which has been recently decided as a place for a showcase of the MHN technology during the 2018 PyeongChang Winter Olympic. The main objective of the test is to investigate the propagation characteristics and performance of the first version of MHN prototype at Yulgok Street, which is expected to give valuable insights into developing the next version of the MHN prototype system to be demonstrated during the 2018.

4.4.3.1 Prototype of MHN system used for the field test

Figure 31 shows the prototypes of MHN system developed in the first year of the project and Table 1 summarizes design requirements of the prototype.

Table 1. Requirements for MHN prototype of the first year

Requirements	Values
Carrier frequency (GHz)	24 ~ 26.5
Number of supported CCs	4

System bandwidth of each CC (MHz)	125
Duplex mode	TDD
Target downlink data rate (Mbps)	1250
Target uplink data rate (Mbps)	180
RF TX/RX paths	1TX/2RX
EIRP (dBm)	36
Maximum TX antenna gain (dBi)	19
Maximum RX antenna gain (dBi)	22
TX power (dBm)	17
Target coverage (curved path)	>300m
Target coverage (straight path)	>500m

Both mRU and mTE testbeds were implemented on Xilinx field programmable gate arrays (FPGAs). In the RF design, four component carriers (CCs), which are contiguously allocated, are employed for carrier aggregation (CA). Since the configuration of the RF transmit (TX) and receive (RX) paths for both mTE and mRU testbeds are 1TX/2RX, both testbeds are equipped with one TX antenna and two RX antennas as shown in Figure 31. For the antenna design, slotted waveguide array antennas with 4x4 and 6x6 radiating elements are employed for TX and RX antennas of the mRU testbeds, respectively, and patch antennas with 4x5 and 5x8 elements are employed for TX and RX antennas of the mTE testbed, respectively. In addition, since it is mandatory to comply with effective isotropic radiated power (EIRP) requirement regulated by Korean government, where the maximum EIRP allowed in the spectrum band for the field test is 36dBm, the TX antenna gains of both mTE and mRU testbeds designed to be 19 dBi and the maximum TX power is 17 dBm. On the other hand, since there is no specific restriction on the RX antenna gain, we set much higher gain of 22dBi to achieve the coverage requirements.

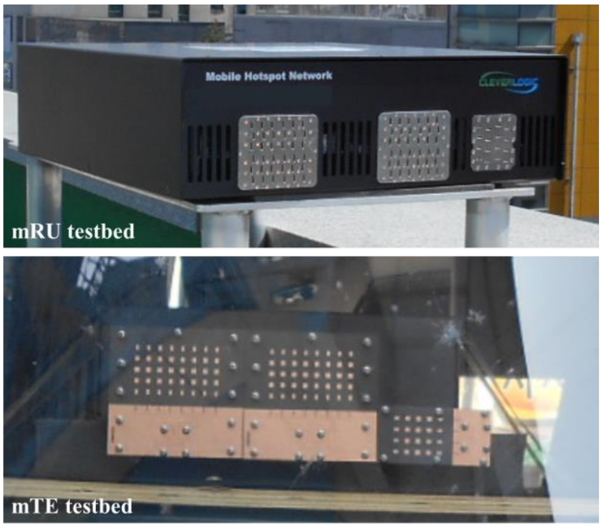

Figure 31 Prototype of MHN system

Due to the antenna configuration of both testbeds, only single antenna transmission is employed at the transmitters of both downlink and uplink, and maximal ratio combining (MRC) technique is used at the receiver side. For the future field trial to be demonstrated during the 2018 PyeongChang Winter Olympics, since two TX antennas at mRU will be available, both spatial frequency block code (SFBC) and open-loop spatial multiplexing (OLSM) techniques will be supported for performance improvement.

4.4.3.2 Test Environments

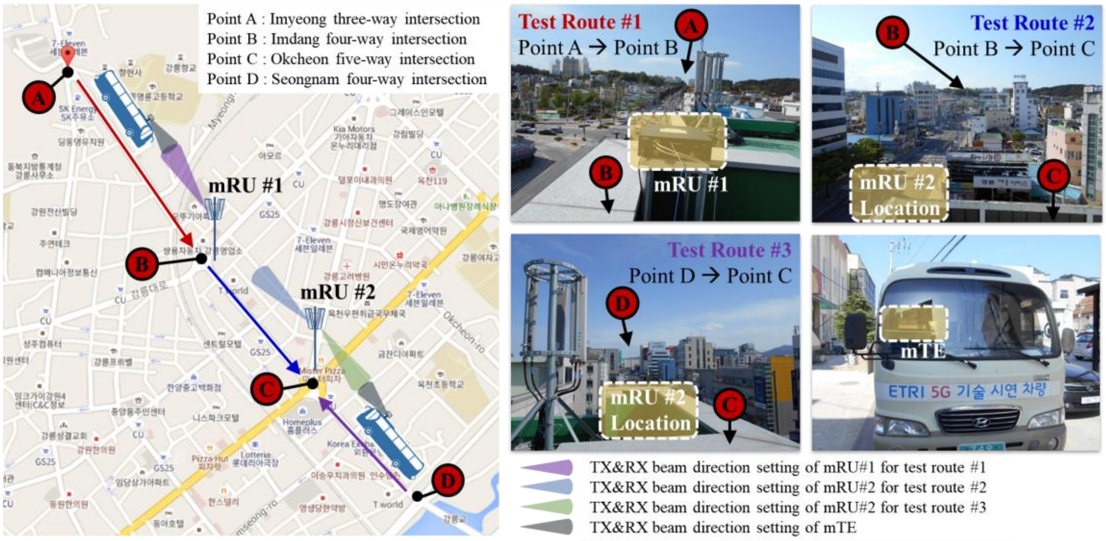

Figure 32 Test Environments (Gangneung IoT Street)

Figure 32 shows the map of the testbed deployment for the preliminary field trial at Yulgok street in Gangneung city. Two mRU testbeds, mRU 1 and mRU 2 are installed on the rooftops of the two buildings located near Imdang four-way intersection and Okcheon five-way intersection, respectively, and a vehicle carrying a testbed of mTE inside drove along the three different paths of the street, which are path 1, path 2 and path 3 as shown in Figure 32. The length of path 1, path 2 and path 3 are 570m, 410m and 400m respectively, and the average velocity of the vehicle was around 60km/h. The first test was carried out as the vehicle moved from point A to point C, and in this case, the antennas direction of mRU 2 was set to point B. When mTE was located at path 1 and path 2, it communicated with mRU 1 and mRU 2 respectively, and since the main objective of the test was to investigate the propagation characteristics and the feasibility of the MHN system in urban scenario, we didn't apply any handover algorithm for simplicity. Instead, when the mTE lost the connection with the serving mRU, it will simply search for the serving mRU and make connection again. The second test was conducted at path 3 starting from point D to point C, and in this case, we had the antenna direction of mRU 2 changed so that the TX beam of the antenna was well aligned with the RX beams of the mTE. The entire test including the test 1 and test 2 was done twice. During the test, various performance metrics (uplink/downlink data rate, block error rate (BLER), signal-to-noise ratio (SNR), etc.) were monitored in real time using a performance monitoring display connected to the mTE testbed. The display also showed the instantaneous time/frequency response of channel and constellation of received signals.

4.4.3.3 Test Results

Figure 33, Figure 34 and Figure 35 show the captured performance monitoring displays of path 1, path 2, path 3, respectively, where green line and blue line represent data rates of downlink and uplink, respectively. The mTE measured the channel qualities based on the received reference signal, and reported them to the network (i.e. mDU) through an uplink so that the scheduler could instantaneously change the modulation and coding schemes (MCSs) for link adaptation. Therefore, as we can see in the three figures, both downlink and uplink data rates fluctuated wildly, which is totally different from what we observed in the field trial at Seoul subway line 8, where around 1.25 Gbps downlink data rate was attainable most of the time except for four handover points where the mTE passed by each mRU. Note that the reason why uplink data rate is much lower than the downlink data rate is the TDD configuration, where the ratio of downlink to uplink is equal to 7.

Figure 33 Test results at path 1

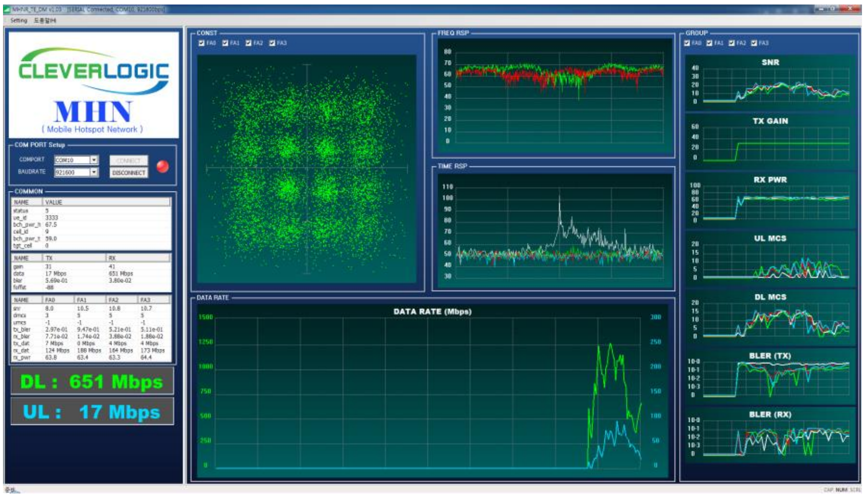

Figure 34 Test results at path 2

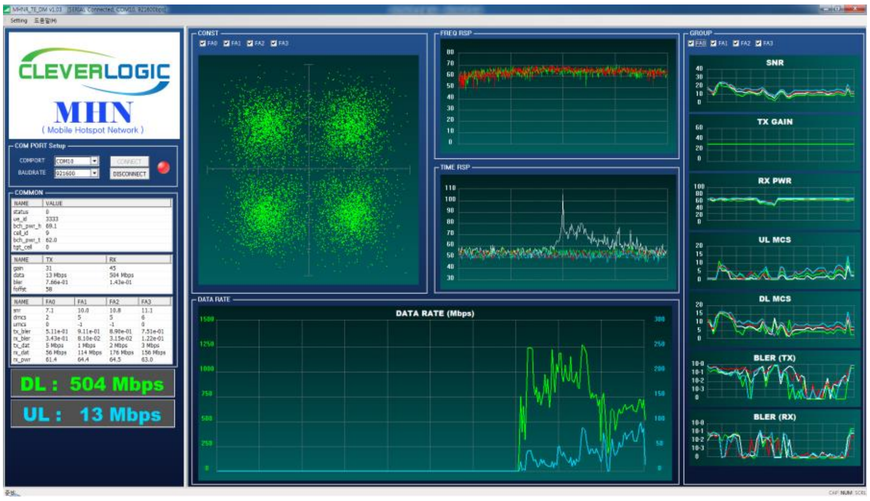

Figure 35 Test results at path 1

More specifically, during the test at path 1 and path 2, the downlink data rates ranging from 800Mbps and 1.25Gbps were observed most of the time and in some regions, downlink data rate dropped even below 500 Mbps due to the misalignment between TX beam and RX beam caused by a slanted direction of the vehicle. In the case of the test at path 3, significant performance degradation was observed in some regions where the performance was lower than 350 Mbps, which is mainly due to blockage of line-of-sight (LoS) signal by obstacles like trees and road signs. This also means that if a larger vehicle drives between an mTE and its serving mRU, the vehicle may act as communication blockages significantly degrading the performance. From the test, we can see that the performance is highly vulnerable to the misalignment between TX and RX beams and the LoS blockage, and the propagation environment in the urban environment is much more severe than that of tunnel environment of Seoul subway line 8, where the surrounding environment is almost fixed, and the tunnel ifself has a waveguide effect providing better channel characteristics as well as link budget. Moreover, since only fixed RF beamforming (BF) was supported at the tranceivers of both mRU and mTE, which is one of the bottlenecks of the current version of prototype system, the performance degradations caused by the aforementioned beam misalignment and signal blockage are inevitable. Alternatively, the next version prototype system to be used for the field trial at Yulgok street during the 2018 PyeongChang Winter Olympics is being designed to configure 2TX/2RX for RF path in mDU testbed enabling OLSM and SFBC for performance improvement while not a fundamental solution to the aforementioned problems. In addition, the next version of prototype system is currently being developed based on the MHN-E system, and it will allow the aggregation of a maximum of eight CCs to attain a total transmission bandwidth of up to 1GHz in order to achieve the maximum downlink data rate of up to 2.5Gbps.

5 Conclusion

D6.4 will be the document that is the one of the outcome of this report.

References

[1] 5GCHAMPION report "Preliminary 5GCHAMPION architecture specifications (IR2.1)," 2016.

[2] 5GCHAMPION Deliverable "Front end design (D3.1)," 2016

[3] 5GCHAMPION report "IR6.1 System level testing of POC phase1 (IR6.1)," 2017